frontiers | Frontiers in Remote Sensing

TYPE Perspective
PUBLISHED 21 October 2022
DOI 10.3389/frsen.2022.1042460

OPEN ACCESS

EDITED BY
Dong Liu,
Hefei Institutes of Physical Science (CAS), China

REVIEWED BY
Tim Kane,
The Pennsylvania State University (PSU), United States

*CORRESPONDENCE
Daniel R. Cremons,
daniel.cremons@nasa.gov

SPECIALTY SECTION
This article was submitted to Lidar Sensing, a section of the journal Frontiers in Remote Sensing

RECEIVED 12 September 2022
ACCEPTED 05 October 2022
PUBLISHED 21 October 2022

CITATION
Cremons DR (2022), The future of lidar in planetary science.
Front. Remote Sens. 3:1042460.
doi: 10.3389/frsen.2022.1042460

The future of lidar in planetary science

Daniel R. Cremons*

Planetary Geology, Geophysics and Geochemistry Laboratory, NASA Goddard Space Flight Center, Greenbelt, MD, United States

Lidar has enabled advances in the knowledge of the Solar System through geophysical and atmospheric studies of the Moon, Mercury, Mars, and several asteroids. The technique will continue to be used to obtain high-precision topographic data from orbit, but new techniques on the horizon are suited to uniquely address fundamental planetary science questions related to the evolution of airless bodies, volatile delivery and sequestration, atmospheric transport, and small body formation and evolution. This perspective highlights the history of lidar in planetary science and identifies several measurement approaches that may be adopted in the coming years.

KEYWORDS

lidar, planetary science, topography, altimetry, reflectance, mapping, volatiles

Introduction

Lidar (light detection and ranging) is a method of measuring a precise range between the instrument and the target using the time-of-flight of a transmitted laser pulse (Gardner, 1982; Sun, 2017; Zhou et al., 2017). When hosted as an orbital payload a lidar provides continuous ranging measurements to the surface, building up topographic profiles along the spacecraft track. Given a suitable orbit and measurement cadence, a topographic map of an entire planet can be constructed with centimeter to meter accuracy and precise geodetic control. Such orbital lidar measurements of the Moon and Mars have provided global topographic maps that stand as foundational datasets for science investigations and exploration efforts. By measuring the transmitted and reflected laser pulse energies, the reflectance of the surface at the laser wavelength can be determined regardless of natural illumination conditions or the thermal state of the surface.

In this perspective I briefly summarize the history of lidar for planetary science applications starting with the Apollo 15 laser altimeter and identify several future techniques and measurement concepts that are relevant to the most pressing planetary science questions. My intention is to highlight how the two fundamental lidar measurements (time of flight and received laser energy) can be used in new ways to provide unique science measurements. I limit this perspective to planetary science lidar investigations and do not focus on the wealth of Earth science lidar missions, ground-based, and airborne investigations, nor do I discuss the use of lidar strictly for navigation and guidance purposes, as is increasingly used for spacecraft docking, terrain relative navigation (TNR), and guidance and control for landing.

TABLE 1 List of planetary lidar instruments and associated science goals.

Mission	Instrument	Target	Science operations	Lidar science goals
Apollo 15, 16, and 17	Apollo Laser Altimeter	The Moon	1971–1972	Measure lunar topography and extract lunar shape parameters
Clementine	Clementine LIDAR	The Moon	1994	Measure lunar topography to study large basin morphology and derive lithospheric properties
Mars Global Surveyor (MGS)	MOLA	Mars	1996–2006	Measure surface topography, surface roughness, albedo, dust, and cloud heights
Mars Polar Lander	Mars Polar Lander LIDAR	Mars	N/A	Quantify dust and aerosols in the lower 3 km of the Mars atmosphere
Near Earth Asteroid Rendezvous (NEAR) - Shoemaker	NLR	Asteroid 433 Eros	2000–2001	Topography for shape and internal structure
Hayabusa	Hayabusa LIDAR	Asteroid 25143 Itokawa	2005	Measure asteroid topography and albedo and contribute to gravity science campaign
Chang'E-1 and Chang'E-2	Chang'E Laser Altimeter	The Moon	2007–2010	Measure global lunar topography
Selenological and Engineering Explorer (SELENE)	LALT	The Moon	2007–2009	Measure global lunar topography
Chandrayaan-1	LLRI	The Moon	2008–2009	Measure lunar topography at high latitudes
Phoenix	MET	Mars	2008	Atmospheric backscatter
Lunar Reconnaissance Orbiter (LRO)	LOLA	The Moon	2009–Present	Measure lunar topography to constrain impact fluxes, model planetary interior, and explore volcanic landforms. Measure albedo to identify potential polar volatiles
MESSENGER	MLA	Mercury	2011–2015	Measure topography of the northern hemisphere, detect physical librations, albedo
Hayabusa2	Hayabusa2 LIDAR	Asteroid 162173 Ryugu	2018–2019	Measure asteroid topography and albedo and contribute to gravity science campaign
OSIRIS-REx	OLA	Asteroid 101955 Bennu	2018–2020	Measure asteroid topography to determine shape and geological origin and evolution
Lunar Flashlight	*Lunar Flashlight*	*The Moon*	*Planned 2023*	*Measure lunar reflectance near the South Pole at 4 infrared wavelengths to constrain water ice*
Jupiter Icy Moons Explorer (JUICE)	*GALA*	*Ganymede*	*Planned 2023*	*Measure Ganymede topography to understand ice tectonics, measure tidal response, understand small-scale roughness, and measure albedo*
BepiColombo	*BELA*	*Mercury*	*Planned 2026*	*Measure topography to determine figure parameters, rotation state, and surface roughness*
Hera	*PALT*	*Asteroid 65803 Didymos*	*Planned 2024*	*Measure asteroid topography and albedo*
Martian Moons eXploration (MMX)	*MMX Lidar*	*Phobos*	*Planned 2025*	*Measure topography for shape model and geological structure of Phobos, measure albedo*

Lidar investigations on planetary science missions

Lidar, also referred to as laser altimetry, has played an important role in planetary science since the Apollo era. The recognition that laser altimetry could provide geodetically controlled, high-precision topographic measurements led to inclusion of the first planetary laser altimeter on the Apollo 15 mission in 1971. The Apollo 15 laser altimeter illuminated 30 m footprints at 30 km spacing during two equatorial orbits (Sjogren and Wollenhaupt, 1973). Even though the surface sampling was sparse by modern standards, this data was critical in developing the lunar shape parameters and constraining the topographic differences between large basins on the Moon, and discovering the far side basin known as the South Pole Aiken Basin (SPA) (Howard et al., 1974; Head, 1976). Following in the footsteps of the three Apollo laser altimeters were the Clementine lidar (Smith et al., 1997) and Lunar Orbiter Laser Altimeter (LOLA) (Smith et al., 2010) built by the National Aeronautics and Space Administration (NASA), the Chang'E-1 (Huixian et al., 2005) and Chang'E-2 (Zuo et al., 2014) lidars built by the China National Space Administration (CNSA), the SELENE laser (LALT) (Araki et al., 2008) built by the Japan Aerospace Exploration Agency (JAXA), and the Chandrayaan-1 laser altimeter (LLRI) (Goswami and Annadurai, 2008) built by the Indian Space Research Organization (ISRO). These instruments were designed to measure global lunar topography and roughness, constrain impact fluxes, explore

volcanic landforms, and measure the lunar albedo at the laser wavelength (1,064 nm). Lidar can geodetically anchor measurements from other payloads such as cameras, spectrometers, and radiometers. Techniques that create topographic maps from imaging including shape from shading and stereophotogrammetry are increasingly common and usually offer higher spatial resolution and coverage at a lower cost than lidar mapping. However, they are reliant upon natural illumination conditions and often have lower vertical resolution than lidar-derived topography. A list of past, present, and planned planetary lidar instruments and their stated science objectives are given in Table 1.

Topography measurements derived from pulsed laser times-of-flight are the primary science product generated from lidar investigations on planetary science missions, and the technologies are relatively mature (Sun et al., 2013). The nine lunar orbital lidar instruments to date have primarily focused on topographic (Araki et al., 2009), slope (Kreslavsky and Head, 2016), and roughness measurements (Kreslavsky et al., 2013), although laser reflectance measurements have been used to look for cold trapped volatiles in polar regions of the Moon and Mercury (Lucey et al., 2014; Hayne et al., 2015; Deutsch et al., 2017). Beyond the Moon, the Mars Orbiter Laser Altimeter (MOLA) (Smith et al., 2001) on the Mars Global Surveyor (MGS) mission provided a global topographic map of Mars, and a similar campaign by the Mercury Laser Altimeter (MLA) (Cavanaugh et al., 2007) on the MESSENGER mission mapped much of the northern hemisphere of Mercury including polar volatile deposits. Four asteroid missions have carried laser altimeters for topography mapping, shape estimation, and landing site characterization: the Near Earth Asteroid Rendezvous (NEAR)–Shoemaker to asteroid 433 Eros (Zuber et al., 1997), the Hayabusa and Hayabusa2 missions to asteroid 25143 Itokawa (Yoshimitsu et al., 2009) and 126,173 Ryugu (Mizuno et al., 2017) respectively, and the Origins, Spectral Interpretation, Resource Identification, Security, Regolith Explorer (OSIRIS-REx) mission to asteroid 101955 Bennu (Daly et al., 2017).

In addition to topography measurements, several lidar systems designed around backscatter measurements have characterized the Mars atmosphere. MOLA made measurements of clouds, dust, and aerosols during its polar orbit, providing the first three-dimensional distribution of Mars clouds (Smith et al., 2001). The Phoenix lander MET lidar (Whiteway et al., 2009) provided backscatter profiles from the surface to several kilometers in altitude at two laser wavelengths: 1,064 nm and the second harmonic of 1,064 nm at 532 nm. The ability to measure distributed aerosol backscatter is a key advantage of lidar over passive atmospheric techniques and has led to its ubiquitous use in Earth atmosphere studies. The Phoenix lidar measured the planetary boundary layer height as a function of time as well as the dust optical extinction and particle size distributions using the two laser wavelengths (Komguem et al., 2013).

Upcoming lidar investigations

Several missions nearing launch will carry laser altimeters using measurement techniques like those that have preceded them, though the targets and prospective mapping campaigns are increasingly ambitious. The BepiColombo mission will use the BepiColombo Laser Altimeter (BELA) (Thomas et al., 2021) to create the first complete lidar map of Mercury. The first ever lidar topography measurements of an outer Solar System body and ice world will be made by the Ganymede Laser Altimeter (GALA) (Enya et al., 2022) on the Jupiter Icy Moons Explorer (JUICE) mission. Phobos will be mapped and sampled using the MMX lidar (Senshu et al., 2021) aboard the Martian Moons Exploration (MMX) mission. Finally, a key test of planetary defence strategies and asteroid orbital dynamics will be supported by the Planetary Laser Altimeter (PALT) (Gordo et al., 2020; Dias et al., 2021) aboard the Hera mission to the asteroid65803 Didymos and its moonlet Dimorphos in support of the Double Asteroid Redirect Mission (DART) (Rivkin et al., 2021).

These four missions all carry laser altimeters designed primarily for time-of-flight measurements, though with several new laser and detector technologies aimed at reducing the size and weight and increasing ranging precision. A notable exception is the upcoming Lunar Flashlight mission (Vinckier et al., 2019; Cohen et al., 2020), which carries a new class of laser reflectometer to measure the lunar surface reflectance at four key infrared wavelengths to constrain the abundance of surface water ice in permanently shadowed regions near the lunar South Pole. This instrument is not designed to provide accurate range measurements, but the quasi-CW operation is not dissimilar to traditional lidar, and we include it in our discussion here. Notably, this will be the first planetary lidar to fly multiple laser systems operating at different wavelengths for surface spectroscopy, which will be discussed further in the next section.

Altimetry and beyond: The future of planetary lidar

The future of lidar in planetary science beyond the missions stated above will involve the utilization of proven techniques at new targets (e.g., the mapping of Ganymede by the GALA instrument), adoption of techniques pioneered in Earth science applications (e.g., gas-phase spectroscopy), and the development of new techniques where lidar can provide unique datasets (e.g., volatile mapping in permanently shadowed regions). In this section, I will discuss three areas in which I believe lidar techniques will evolve in the coming years and decades to uniquely tackle challenging planetary science

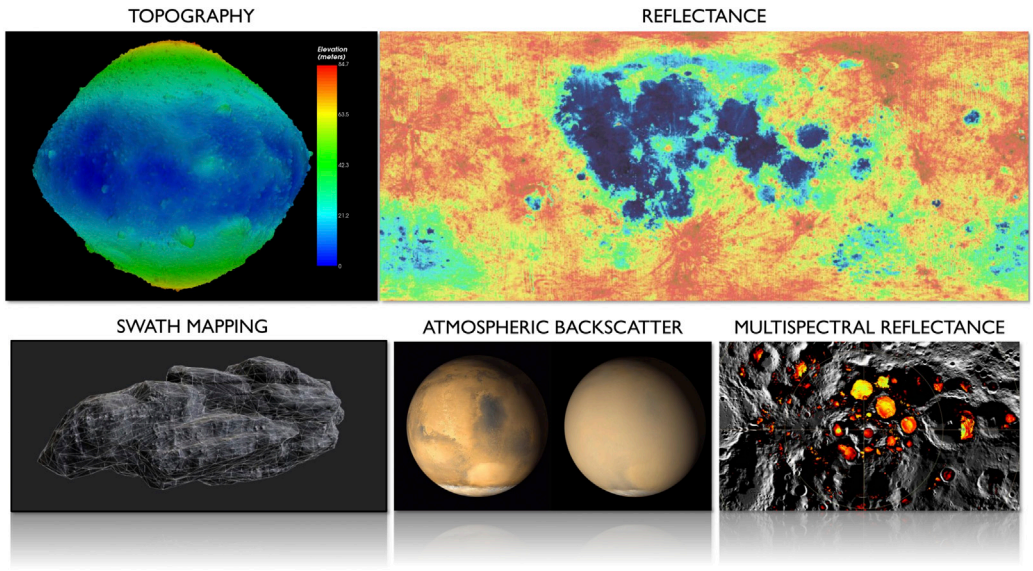

FIGURE 1
Overview of lidar investigations in planetary science. Past and current work focuses on topography (OLA-derived topographic map of asteroid 101955 Bennu, top left) and single-wavelength reflectance or normal albedo (LOLA-derived normal albedo map of the Moon, top right). Several future techniques on the horizon include swath-mapping lidar for high spatial resolution and coverage (surface terrain mapping, bottom left), atmospheric backscatter, trace gas, and Doppler measurements (Mars global dust storm, center bottom), and multispectral reflectance spectroscopy (permanently shadowed regions at the lunar South Pole, bottom right).

questions (Figure 1). I stress that other nascent and mature lidar techniques exist that can also be readily applied to planetary science questions, and this list should be not taken as exhaustive or even comprehensive.

Topography

Lidar will continue to be a method of choice to create geodetically controlled topographic maps of planetary targets from orbit and will likely also expand to use on surface assets such as landers, rovers, or astronaut-deployed instruments. Scientific exploration of the Moon will focus on the South Pole as the region of interest due to visibility to Earth, presence of *in situ* resources, and select locations of almost constant illumination (Smith et al., 2020). Outside of these highly illuminated regions the terrain is an ever-changing mixture of partial or permanent shadow, which presents significant challenges to mapping with passive imagery. The permanently shadowed regions (PSRs) can experience darkness on geologic timescales (billions of years), preserving volatile species *via* cold trapping (Zhang and Paige, 2009; Mazarico et al., 2011). PSRs are sites of high scientific interest for their ability to preserve volatiles from early Solar System history and provide *in situ* resources for exploration. Comprehensive mapping of the South Pole to assess illumination and hazard conditions, as well as further investigate these dark regions on the exploration scale (meters) is a task well-suited for lidar, though high resolution maps will require new technologies that improve the spatial resolution over present approaches.

Two techniques that can enable higher resolution topographic mapping are scanning lidar and swath mapping lidar. Scanning lidar, which was first used in a planetary context on the OSIRIS-REx laser altimeter, uses a beam pointing mechanism to move a small laser footprint across the lidar field of view (Raj et al., 2020). Beam pointing mechanisms currently in use include optomechanical (mirrors and prisms such as the mirror on OLA), electromechanical and microelectromechanical systems (MEMS) (Kasturi et al., 2016), and nascent solid state mechanisms including optical phase arrays (Bhargava et al., 2019), photonic waveguides (Abe et al., 2018), and adaptive wavelength scanning (Yang et al., 2022). Scanning lidar is becoming commonplace in industrial and automotive lidar applications (Thakur, 2016) but has recently entered the aerospace sector (Nimelman et al., 2005; Daly et al., 2017; Bo et al., 2019). Terrestrial scanning lidar has been widely used in Earth science and surveying applications to create high-resolution digital elevation models (DEMs). Similar approaches will likely be applied to the lunar South Pole in support of NASA's Artemis campaign in coming years. From orbit, scanning lidar allows for a broader cross-track area to be sampled, which can increase mapping coverage and reduce repeat sampling of the same terrain.

Swath mapping lidar involves the use of pixelated detectors that record a time-of-flight for each pixel, giving contiguous coverage of the detector field of view with tens to hundreds of simultaneous measurements (Glennie et al., 2013; Meigs, 2013; Sun et al., 2021). The transition from a few beams, as was used on LOLA, to dozens of adjacent pixels will lead to orders of magnitude increases in spatial resolution and coverage, although to maintain the link margin an increase in laser power is often required. These two techniques, separately or in tandem, can lead to higher resolution topographic maps to resolve fine scale surface roughness, provide improved geodetic measurements of tidal response, and identify new surface morphologies across the Solar System.

Reflectance spectroscopy

A crucial aspect of lidar measurements is that the angle between the incidence of light on the surface and the emission of light to the receiver is zero, meaning the observation geometry is always uniform. This makes global and time-of-day comparisons between measurements simpler and more robust than for passive measurements which require thermal, surface slope, and illumination correction. In addition, the finite laser pulses enable the removal of background illumination from the Sun or thermal emission from the surface or atmosphere by measuring the signal between laser pulses (i.e., the noise) This last aspect is particularly advantageous for questions related to volatile delivery, migration, and retention; processes which are likely dependent on surface temperature and solar illumination (Lucey et al., 2021).

The uniform measurement geometry and active laser source enables high signal to noise ratio regardless of solar illumination and perform better over the most scientifically desirable shadowed terrain. Spectroscopic lidar operates by measuring the surface reflectance both on and off infrared absorption features for the volatile or mineral species of interest. Depending on the choice of laser wavelengths, measurements of the surface reflectance within PSRs would constrain the abundance of surface volatiles including water ice, carbon dioxide, and organics, as well as water or hydroxyl ions bound within minerals or adsorbed on the surface. As with other lidars, spectroscopic lidar could be used to create a topographic map that is directly tied to the volatile abundance measurements. Spectroscopic lidar would excel in planetary applications involving unilluminated or rapidly changing illumination conditions where passive techniques suffer from low signal and uncertainty in thermal correction. When used in combination with passive remote sensing instruments, a high-resolution, global, low-bias dataset can be generated. This concept was proposed for the Lunar Volatiles Orbiter, which combined an imaging spectrometer with a spectroscopic lidar (Lucey et al., 2017). Global spectroscopic reflectance measurements taken at all latitudes, times of day, and surface temperatures would offer unique insights into the generation, migration, sequestration, and destruction of water, hydroxyl, and other volatiles.

Atmospheric absorption and doppler-resolved backscatter

The narrow spectral linewidth of lidar laser transmitters may enable gas-phase spectroscopy in planetary atmospheres using either light reflected from the surface or backscattered from the atmosphere. Differential absorption lidar (Browell et al., 1998) involves measuring the relative absorption of laser wavelengths both on and off absorption lines from an atmospheric constituent of choice. Earth science applications of this technique have focused on measuring the abundance of ozone (Browell, 1989), water vapor (Spuler et al., 2015; Nehrir et al., 2017), carbon dioxide (Koch et al., 2004; Abshire et al., 2010), and methane (Kiemle et al., 2014, 2011). Potential planetary science applications include measurements of water vapor and elusive methane at Mars, methane and tholins at Titan, and plume backscatter measurements at Enceladus. Extremely narrow laser linewidths in the megahertz regime enable Doppler-resolved backscatter profile measurements that can be converted into vector wind profiles (Chanin et al., 1989; Korb et al., 1998; Cremons et al., 2020). There is a paucity of direct wind speed measurements in planetary atmospheres, and only recently has the ADM-Aeolus mission (Reitebuch, 2012; Witschas et al., 2020) provided global wind measurements of Earth. Wind measurements on Mars or Titan would constrain energy and material transport mechanisms and haze formation, as well as aid in understanding the modern Mars atmosphere including the development of the polar caps and how wind shapes the landscape (MEPAG, 2020). Compared to high-resolution topography and reflectance spectroscopy, the differential absorption and Doppler techniques face greater implementation challenges at present due to the very narrow laser linewidths and spectral receiver stability required while under challenging operational conditions.

Summary

Lidar has been a cornerstone remote sensing technique throughout the history of planetary science by providing foundational datasets in the form of global topographic maps for the Moon, Mercury, Mars, and several asteroids. The fundamental measurement capabilities of ranging and laser reflectance will continue to be utilized in the near term on new and exciting planetary targets. Maturing lidar technologies from other industries will continue to lower the cost of simple rangefinders for inclusion on lower cost SmallSat and CubeSat missions and cases

where ranges in the tens to hundreds of meters are sufficient. Looking further ahead, advancements in laser and detector technology will result in a leap in spatial resolution and coverage. The use of new and multiple laser wavelengths will turn lidar into a spectroscopic technique that can measure regions in shadow with uniform viewing geometry irrespective of the thermal state of the surface. Although more technically challenging, narrow-linewidth lidar at Mars or Titan could provide high-resolution spectroscopy of key atmospheric constituents or provide vertical wind profiles for the first time.

Data availability statement

Publicly available datasets were analyzed in this study. This data can be found here: The lidar-based DTM for asteroid 101,955 Bennu is the OLA V20 PTM which is described in Daly, M. G. et al., 2020, Hemispherical Differences in the Shape and Topography of Asteroid (101955) Bennu, Science Advances, 6 (41), eabd3649. The LOLA-derived albedo map and PSR maps were generated using the ACT Lunar QuickMap and data products described in Lemelin, M., P. G. Lucey, G. A. Neumann, E. M. Mazarico, M. K. Barker, A. Kakazu, D. Trang, D. E. Smith, and M. T. Zuber. "Improved calibration of reflectance data from the LRO Lunar Orbiter Laser Altimeter (LOLA) and implications for space weathering." Icarus 273 (2016): 315-328 and Diviner-derived polar summer maximum temperature as described in Williams, J.-P., et al. (2019). Seasonal polar temperatures on the Moon. Journal of Geophysical Research: Planets, 124, 2505–2,521. https://doi.org/10.1029/2019JE006028.

Author contributions

DC: Conceptualization, investigation, writing—original draft preparation, writing—editing and revising, visualization. All authors have read and agreed to the published version of the manuscript.

Funding

This study was supported by the NASA Goddard Space Flight Center Internal Research and Development Program.

Conflict of interest

The author declares that the research was conducted in the absence of any commercial or financial relationships that could be construed as a potential conflict of interest.

Publisher's note

All claims expressed in this article are solely those of the authors and do not necessarily represent those of their affiliated organizations, or those of the publisher, the editors and the reviewers. Any product that may be evaluated in this article, or claim that may be made by its manufacturer, is not guaranteed or endorsed by the publisher.

References

Abe, H., Takeuchi, M., Takeuchi, G., Ito, H., Yokokawa, T., Kondo, K., et al. (2018). Two-dimensional beam-steering device using a doubly periodic Si photonic-crystal waveguide. *Opt. Express* 26, 9389. doi:10.1364/OE.26.009389

Abshire, J. B., Riris, H., Allan, G. R., Weaver, C. J., Mao, J., Sun, X., et al. (2010). Pulsed airborne lidar measurements of atmospheric CO2 column absorption. *Tellus B Chem. Phys. Meteorology* 62, 770–783. doi:10.1111/j.1600-0889.2010.00502.x

Araki, H., Tazawa, S., Noda, H., Ishihara, Y., Goossens, S., Sasaki, S., et al. (2009). Lunar global shape and polar topography derived from kaguya-LALT laser altimetry. *Science* 323, 897–900. doi:10.1126/science.1164146

Araki, H., Tazawa, S., Noda, H., Tsubokawa, T., Kawano, N., and Sasaki, S. (2008). Observation of the lunar topography by the laser altimeter LALT on board Japanese lunar explorer SELENE. *Adv. Space Res.* 42, 317–322. doi:10.1016/j.asr.2007.05.042

Bhargava, P., Kim, T., Poulton, C. V., Notaros, J., Yaacobi, A., Timurdogan, E., et al. (2019). "Fully integrated coherent LiDAR in 3D-integrated silicon photonics/65nm CMOS," in 2019 Symposium on VLSI Circuits. Presented at the 2019 Symposium on VLSI Circuits, Kyoto, Japan, 09-14 June 2019 (IEEE), C262–C263. doi:10.23919/VLSIC.2019.8778154

Bo, L., Yang, Y., and Shuo, J. (2019). Review of advances in LiDAR detection and 3D imaging. *Opto-Electronic Eng.* 46, 190167–190171.

Browell, E. V. (1989). Differential absorption lidar sensing of ozone. *Proc. IEEE* 77, 419–432. doi:10.1109/5.24128

Browell, E. V., Ismail, S., and Grant, W. B. (1998). Differential absorption lidar (DIAL) measurements from air and space. *Appl. Phys. B Lasers Opt.* 67, 399–410. doi:10.1007/s003400050523

Cavanaugh, J. F., Smith, J. C., Sun, X., Bartels, A. E., Ramos-Izquierdo, L., Krebs, D. J., et al. (2007). The mercury laser altimeter instrument for the MESSENGER mission. *Space Sci. Rev.* 131, 451–479. doi:10.1007/s11214-007-9273-4

Chanin, M. L., Garnier, A., Hauchecorne, A., and Porteneuve, J. (1989). A Doppler lidar for measuring winds in the middle atmosphere. *Geophys. Res. Lett.* 16, 1273–1276. doi:10.1029/GL016i011p01273

Cohen, B. A., Hayne, P. O., Greenhagen, B., Paige, D. A., Seybold, C., and Baker, J. (2020). Lunar flashlight: Illuminating the lunar South Pole. *IEEE Aerosp. Electron. Syst. Mag.* 35, 46–52. doi:10.1109/MAES.2019.2950746

Cremons, D. R., Abshire, J. B., Sun, X., Allan, G., Riris, H., Smith, M. D., et al. (2020). Design of a direct-detection wind and aerosol lidar for Mars orbit. *CEAS Space J.* 12, 149–162. doi:10.1007/s12567-020-00301-z

Daly, M. G., Barnouin, O. S., Dickinson, C., Seabrook, J., Johnson, C. L., Cunningham, G., et al. (2017). The OSIRIS-REx laser altimeter (OLA) investigation and instrument. *Space Sci. Rev.* 212, 899–924. doi:10.1007/s11214-017-0375-3

Deutsch, A. N., Neumann, G. A., and Head, J. W. (2017). New evidence for surface water ice in small-scale cold traps and in three large craters at the north polar region of Mercury from the Mercury Laser Altimeter. *Geophys. Res. Lett.* 44, 9233–9241. doi:10.1002/2017GL074723

Dias, N. G., Arribas, B. N., Gordo, P., Sousa, T., Marinho, J., Melicio, R., et al. (2021). LIDAR altimeter conception for HERA spacecraft. *Aircr. Eng. Aerosp. Technol.* 93, 1018–1028. doi:10.1108/aeat-12-2020-0300

Enya, K., Kobayashi, M., Kimura, J., Araki, H., Namiki, N., Noda, H., et al. (2022). The Ganymede laser altimeter (GALA) for the jupiter icy Moons explorer (JUICE): Mission, science, and instrumentation of its receiver modules. *Adv. Space Res.* 69, 2283–2304. doi:10.1016/j.asr.2021.11.036

Gardner, C. S. (1982). Target signatures for laser altimeters: An analysis. *Appl. Opt.* 21, 448–453. doi:10.1364/ao.21.000448

Glennie, C. L., Carter, W. E., Shrestha, R. L., and Dietrich, W. E. (2013). Geodetic imaging with airborne LiDAR: The earth's surface revealed. *Rep. Prog. Phys.* 76, 086801. doi:10.1088/0034-4885/76/8/086801

Gordo, P., Dias, N. G., Couto, B., Arribas, B. N., Amorim, A., Livio, B., et al. (2020). "Planetary altimeter for HERA development," in Proc. Europlanet Science Congress (EPSC), September 29, 2022, 1–4.

Goswami, J. N., and Annadurai, M. (2008). Chandrayaan-1 mission to the moon. *Acta Astronaut.* 63, 1215–1220. doi:10.1016/j.actaastro.2008.05.013

Hayne, P. O., Hendrix, A., Sefton-Nash, E., Siegler, M. A., Lucey, P. G., Retherford, K. D., et al. (2015). Evidence for exposed water ice in the Moon's south polar regions from Lunar Reconnaissance Orbiter ultraviolet albedo and temperature measurements. *Icarus* 255, 58–69. doi:10.1016/j.icarus.2015.03.032

Head, J. W. (1976). Lunar volcanism in space and time. *Rev. Geophys.* 14, 265. doi:10.1029/RG014i002p00265

Howard, K. A., Wilhelms, D. E., and Scott, D. H. (1974). Lunar basin formation and highland stratigraphy. *Rev. Geophys.* 12, 309. doi:10.1029/RG012i003p00309

Huixian, S., Shuwu, D., Jianfeng, Y., Ji, W., and Jingshan, J. (2005). Scientific objectives and payloads of Chang'E-1 lunar satellite. *J. Earth Syst. Sci.* 114, 789–794. doi:10.1007/bf02715964

Kasturi, A., Milanovic, V., Atwood, B. H., and Yang, J. (2016). "UAV-borne lidar with MEMS mirror-based scanning capability," in *Laser radar technology and applications XXI* (SPIE), 206–215.

Kiemle, C., Kawa, S. R., Quatrevalet, M., and Browell, E. V. (2014). Performance simulations for a spaceborne methane lidar mission. *J. Geophys. Res. Atmos.* 119, 4365–4379. doi:10.1002/2013JD021253

Kiemle, C., Quatrevalet, M., Ehret, G., Amediek, A., Fix, A., and Wirth, M. (2011). Sensitivity studies for a space-based methane lidar mission. *Atmos. Meas. Tech.* 4, 2195–2211. doi:10.5194/amt-4-2195-2011

Koch, G. J., Barnes, B. W., Petros, M., Beyon, J. Y., Amzajerdian, F., Yu, J., et al. (2004). Coherent differential absorption lidar measurements of CO_2. *Appl. Opt.* 43, 5092. doi:10.1364/AO.43.005092

Komguem, L., Whiteway, J. A., Dickinson, C., Daly, M., and Lemmon, M. T. (2013). Phoenix LIDAR measurements of Mars atmospheric dust. *Icarus* 223, 649–653. doi:10.1016/J.ICARUS.2013.01.020

Korb, C. L., Gentry, B. M., Li, S. X., and Flesia, C. (1998). Theory of the double-edge technique for Doppler lidar wind measurement. *Appl. Opt.* 37, 3097. doi:10.1364/ao.37.003097

Kreslavsky, M. A., Head, J. W., Neumann, G. A., Rosenburg, M. A., Aharonson, O., Smith, D. E., et al. (2013). Lunar topographic roughness maps from Lunar Orbiter Laser Altimeter (LOLA) data: Scale dependence and correlation with geologic features and units. *Icarus* 226, 52–66. doi:10.1016/j.icarus.2013.04.027

Kreslavsky, M. A., and Head, J. W. (2016). The steepest slopes on the moon from lunar orbiter laser altimeter (LOLA) data: Spatial distribution and correlation with geologic features. *Icarus* 273, 329–336. doi:10.1016/j.icarus.2016.02.036

Lucey, P. G., Neumann, G. A., Riner, M. A., Mazarico, E., Smith, D. E., Zuber, M. T., et al. (2014). The global albedo of the Moon at 1064 nm from LOLA. *J. Geophys. Res. Planets* 119, 1665–1679. doi:10.1002/2013JE004592

Lucey, P. G., Petro, N., Hurley, D., Farrell, W., Prem, P., Costello, E., et al. (2021). Volatile interactions with the lunar surface. *Geochemistry* 82, 125858. doi:10.1016/j.chemer.2021.125858

Lucey, P., Petro, N., Hurley, D., Farrell, W., Sun, X., Green, R., et al. (2017). "The lunar volatiles orbiter: A lunar discovery mission concept," in 2017 Annual Meeting of the Lunar Exploration Analysis Group, Columbia, MD, October 11, 2017, 5048.

Mazarico, E., Neumann, G., Smith, D., Zuber, M., and Torrence, M. (2011). Illumination conditions of the lunar polar regions using LOLA topography. *Icarus* 211, 1066–1081. doi:10.1016/j.icarus.2010.10.030

Meigs, A. (2013). Active tectonics and the LiDAR revolution. *Lithosphere* 5, 226–229. doi:10.1130/RF.L004.1

MEPAG (2020). Mars scientific goals, objectives, investigations, and priorities: 2020. White paper. Editor D. Banfield (Mars Exploration Program Analysis Group (MEPAG)), 89. Available at: https://mepag.jpl.nasa.gov/reports.cfm.

Mizuno, T., Kase, T., Shiina, T., Mita, M., Namiki, N., Senshu, H., et al. (2017). Development of the laser altimeter (LIDAR) for Hayabusa2. *Space Sci. Rev.* 208, 33–47. doi:10.1007/s11214-015-0231-2

Nehrir, A. R., Kiemle, C., Lebsock, M. D., Kirchengast, G., Buehler, S. A., Löhnert, U., et al. (2017). Emerging technologies and synergies for airborne and space-based measurements of water vapor profiles. *Surv. Geophys.* 38, 1445–1482. doi:10.1007/s10712-017-9448-9

Nimelman, M., Tripp, J., Bailak, G., and Bolger, J. (2005). "Spaceborne scanning lidar system (SSLS)," in *Spaceborne sensors II* (SPIE), 73–82.

Raj, T., Hashim, F. H., Huddin, A. B., Ibrahim, M. F., and Hussain, A. (2020). A survey on LiDAR scanning mechanisms. *Electronics* 9, 741. doi:10.3390/electronics9050741

O. Reitebuch (Editor) (2012). "The spaceborne wind lidar mission ADM-aeolus," *Atmospheric physics* (Springer-Verlag Berlin Heidelberg), 815–827. doi:10.1007/978-3-642-30183-4_49

Rivkin, A. S., Chabot, N. L., Stickle, A. M., Thomas, C. A., Richardson, D. C., Barnouin, O., et al. (2021). The double asteroid redirection test (DART): Planetary defense investigations and requirements. *Planet. Sci. J.* 2, 173. doi:10.3847/PSJ/ac063e

Senshu, H., Mizuno, T., Umetani, K., Nakura, T., Konishi, A., Ogawa, A., et al. (2021). Light detection and ranging (LIDAR) laser altimeter for the Martian Moons Exploration (MMX) spacecraft. *Earth Planets Space* 73, 219–226. doi:10.1186/s40623-021-01537-7

Sjogren, W., and Wollenhaupt, W. (1973). Lunar shape via the Apollo laser altimeter. *Science* 179, 275–278. doi:10.1126/science.179.4070.275

Smith, D. E., Zuber, M. T., Frey, H. V., Garvin, J. B., Head, J. W., Muhleman, D. O., et al. (2001). Mars orbiter laser altimeter: Experiment summary after the first year of global mapping of mars. *J. Geophys. Res.* 106, 23689–23722. doi:10.1029/2000JE001364

Smith, D. E., Zuber, M. T., Jackson, G. B., Cavanaugh, J. F., Neumann, G. A., Riris, H., et al. (2010). The lunar orbiter laser altimeter investigation on the lunar reconnaissance orbiter mission. *Space Sci. Rev.* 150, 209–241. doi:10.1007/s11214-009-9512-y

Smith, D. E., Zuber, M. T., Neumann, G. A., and Lemoine, F. G. (1997). Topography of the moon from the clementine lidar. *J. Geophys. Res.* 102, 1591–1611. doi:10.1029/96JE02940

Smith, M., Craig, D., Herrmann, N., Mahoney, E., Krezel, J., McIntyre, N., et al. (2020). "The Artemis program: An overview of NASA's activities to return humans to the moon," in 2020 IEEE Aerospace Conference, Big Sky, MT, USA, 07-14 March 2020 (IEEE), 1–10.

Spuler, S. M., Repasky, K. S., Morley, B., Moen, D., Hayman, M., and Nehrir, A. R. (2015). Field-deployable diode-laser-based differential absorption lidar (DIAL) for profiling water vapor. *Atmos. Meas. Tech.* 8, 1073–1087. doi:10.5194/amt-8-1073-2015

Sun, X., Abshire, J. B., McGarry, J. F., Neumann, G. A., Smith, J. C., Cavanaugh, J. F., et al. (2013). Space lidar developed at the NASA goddard space flight center—the first 20 years. *IEEE J. Sel. Top. Appl. Earth Obs. Remote Sens.* 6, 1660–1675. doi:10.1109/JSTARS.2013.2259578

Sun, X., Cremons, D. R., Mazarico, E., Yang, G., Abshire, J. B., Smith, D. E., et al. (2021). Small all-range lidar for asteroid and comet core missions. *Sensors* 21, 3081. doi:10.3390/s21093081

Sun, X. (2017). "Lidar sensors from space," in *Comprehensive remote sensing* (Oxford: Elsevier), 412–432. doi:10.1016/B978-0-12-409548-9.10327-6

Thakur, R. (2016). Scanning LIDAR in advanced driver assistance systems and beyond: Building a road map for next-generation LIDAR technology. *IEEE Consum. Electron. Mag.* 5, 48–54. doi:10.1109/MCE.2016.2556878

Thomas, N., Hussmann, H., Spohn, T., Lara, L., Christensen, U., Affolter, M., et al. (2021). The BepiColombo laser altimeter. *Space Sci. Rev.* 217, 25–62. doi:10.1007/s11214-021-00794-y

Vinckier, Q., Hardy, L., Gibson, M., Smith, C., Putman, P., Hayne, P. O., et al. (2019). Design and characterization of the multi-band SWIR receiver for the lunar flashlight CubeSat mission. *Remote Sens.* 11, 440. doi:10.3390/rs11040440

Whiteway, J., Daly, M., Carswell, A., Duck, T., Dickinson, C., Komguem, L., et al. (2009). Lidar on the phoenix mission to Mars. *J. Geophys. Res.* 113, E00A08. doi:10.1029/2007JE003002

Witschas, B., Lemmerz, C., Geiß, A., Lux, O., Marksteiner, U., Rahm, S., et al. (2020). First validation of Aeolus wind observations by airborne Doppler wind lidar measurements. *Atmos. Meas. Tech.* 13, 2381–2396. doi:10.5194/amt-13-2381-2020

Yang, G., Harding, D., Chen, J. R., Stephen, M., Sun, X., Li, H., et al. (2022). "Adaptive wavelength scanning lidar (AWSL) for 3D mapping from space," in IGARSS 2022 - 2022 IEEE international geoscience and remote sensing symposium, 4268–4271. https://doi.org/10.1109/IGARSS46834.2022.9884418.

Yoshimitsu, T., Kawaguchi, J., Hashimoto, T., Kubota, T., Uo, M., Morita, H., et al. (2009). Hayabusa-final autonomous descent and landing based on target marker tracking. *Acta Astronaut.* 65, 657–665. doi:10.1016/J.ACTAASTRO.2009.01.074

Zhang, J. A., and Paige, D. A. (2009). Cold-trapped organic compounds at the poles of the moon and Mercury: Implications for origins. *Geophys. Res. Lett.* 36, L16203. doi:10.1029/2009GL038614

Zhou, H., Chen, Y., Hyyppä, J., and Li, S. (2017). An overview of the laser ranging method of space laser altimeter. *Infrared Phys. Technol.* 86, 147–158. doi:10.1016/j.infrared.2017.09.011

Zuber, M. T., Smith, D. E., Cheng, A. F., and Cole, T. D. (1997). The NEAR laser ranging investigation. *J. Geophys. Res.* 102, 23761–23773. doi:10.1029/97JE00890

Zuo, W., Li, C., and Zhang, Z. (2014). Scientific data and their release of Chang'E-1 and Chang'E-2. *Chin. J. Geochem.* 33, 24–44. doi:10.1007/s11631-014-0657-3